Phase transformations evaluation on a UNS S31803 duplex stainless steel based on nondestructive testing

Edgard de Macedo Silva [a], Victor Hugo Costa de Albuquerque [b], Josinaldo Pereira Leite [b], Antonio Carlos Gomes Varela [b], Elineudo Pinho de Moura [c], João Manuel R.S. Tavares [d],*

[a] Centro federal de Educação Tecnológica da Paraíba (CEFET PB), Área da Indústria, Avenida 1° de Maio, 720 - 58015-430 - João Pessoa/PB, Brazil
[b] Universidade Federal da Paraíba (UFPB), Departamento de Engenharia Mecânica (DEM), Cidade Universitária, S/N - 58059-900 - João Pessoa/PB, Brazil
[c] Universidade Federal do Ceará (UFC), Departamento de Engenharia Metalúrgica e de Materiais, Campus do Pici, Bloco 715, 60455-760 - Fortaleza/CE, Brazil
[d] Faculdade de Engenharia da Universidade do Porto (FEUP), Departamento de Engenharia Mecânica e Gestão Industrial (DEMEGI)/Instituto de Engenharia Mecânica
e Gestão Industrial (INEGI), Rua Dr. Roberto Frias, s/n, 4200-465 Porto, Portugal

ARTICLE INFO

ABSTRACT

Duplex stainless steel presents special mechanical properties such as, for example, mechanical and corrosion strength, becoming competitive in relation to the other types of stainless steel. One of the great problems of duplex stainless steel microstructural changes study is related to embrittlement above 300 °C, with the precipitation of the α' phase occurring over the ferritic microstructure. Aiming to characterise embrittlement of duplex stainless steel, hardening kinetics, from 425 to 475 °C, was analysed through the speed of sound, Charpy impact energy, X-ray diffraction, hardness and microscopy parameters. The presence of two hardening stages, detected through the speed of sound, was observed, one being of brittle characteristic and the other ductile. Moreover, the speed of sound showed a direct correlation with the material's hardness. Thus, it is concluded that the speed of sound is a promising nondestructive parameter to follow-up embrittlement in duplex stainless steel.

1. Introduction

Materials embrittlement study has been performed through ultrasonic measurement, sound attenuation analysis, speed of sound and backscattered signal, as well as spectrum analysis. Microstructual variations cause the scattering of the sound wave causing an increased attenuation of the material. This technique's field of operation depends on the knowledge of the material's sound attenuation coefficient. However, the speed of sound variation is sensitive to the material's embrittlement. The application of this technique in practical situations depends on the accuracy of the material's thickness measurement. A way to eliminate the thickness measurement limitation is to determine a transversal and longitudinal relation between speeds, however the determination of this relation reduces the method's sensitivity [1].

Another used technique is spectrum analysis that is caused by the reflections of sound on the material's microstructure. This technique is based on the analysis of the signal's frequency domain and its correlation with the microstructure. The studied interaction can be evaluated by the frequency distribution alteration of the transmitted or scattered ultrasonic pulse signal [2].

The propagation of ultrasonic waves in polycrystalline materials are subject to interact with microstructural components such as specks, inclusions, porosities, microcracks, corrosion, among others, causing sound attenuations and variation in the speed of sound propagation on the material in analysis [3–5].

The wave propagation speed and energy losses through interactions with the microstructure are the fundamental factors of the material's ultrasonic characterisation. These parameters may be used to determine elastic constants, microstructural analysis, texture, among other mechanical characteristics [6].

The propagation rate of ultrasonic waves in any polycrystalline material is controlled by the material's elasticity module and density, being influenced by the microstructure, the change of the specks' elasticity module through the orientation of the specks' texture and second phase particles [6].

* Corresponding author. Tel.: +351 22 5081487; fax: +351 22 5081445.
E-mail addresses: edgard@cefetpb.edu.br (E. de Macedo Silva), victor.albuquerque@fe.up.pt (V.H.C. de Albuquerque), josinaldo@ct.ufpb.br (J.P. Leite), varela@cefetpb.edu.br (A.C.G. Varela), elineudo@pq.cnpq.br (E.P.d. Moura), tavares@fe.up.pt (J.M.R.S. Tavares).

Other mechanical tests such as, for example, hardness measurement and Charpy impact testing are also used to evaluate susceptibility in duplex stainless steel [7].

Badidi et al. [8], have studied the effect of microstructural variation of martensite to ferrite–perlite for steel with 0.4% of carbon, aimed at correlating the sound speed values with the material's hardness. It has obtained a direct correlation between hardness and sound speed. This relationship between sound speed and hardness was verified in Tane et al. [9], work, where duplex stainless steel JIS-SCS14A (CF8M) from 400 °C with aging of 10 h was used as a sample.

As well as Badidi et al., [8], Shigeyuki, [10], and Shigeyuki et al., [11], have studied the same relationship between speed and the material's hardness using samples of duplex stainless steel aged at 475 °C. However, Shigeyuki did not obtain a direct relation between the sound speed values with the materials' hardness and with an inverse correlation being observed.

Palanichamy [12], studied the application of sound speed measurements for determining the speck size of austenitic stainless steels, since the materials' speck size influences countless mechanical properties, such as: mechanical, tensile and corrosion strength, yield point and toughness, among others. It was observed that the sound speed is affected by the speck size, that is, an increase in speck size implies that the ultrasonic waves will take longer to cover the material's densities, causing the reduction in sound speed.

There are several variables to be analysed concerning the use of ultrasonic testing such as a microstructural inspection technique. A study of these nondestructive techniques will result in the development of procedures to follow-up operating pipes and, consequently, determining the best time to halt service for maintenance and the prevention of disasters which cause social and economic problems.

This research work aims at studying the kinetics of the precipitation of the spinodal decomposition α' phase on the embrittlement of duplex stainless steel (DSS) UNS S31803 from 425 to 475 °C. Thus, it is possible to develop a nondestructive procedure to forecast, when operating, the best time to exchange or maintain duplex stainless steel piping. To do so, it is necessary to characterise, initially, the transformations which occur in steel through destructive testing such as, for example, X-ray diffraction, energy absorbed through Charpy impact and hardness. With the results obtained through these destructive tests, was possible to analyze the potentiality and efficiency of the ultrasonic test in the characterization of phases transformation kinetics of the samples considered.

2. Materials and methods

The phase changes from 425 to 475 °C for a duplex stainless steel UNS S31803, whose chemical composition is in Table 1, were studied.

To carry out the experimental part of our work, first it was necessary to apply thermal treatment on the DSS sample, aimed at evaluating the aging kinetics according to the time and temperature exposure in the oven. In this context, the samples used were aged in an electric resistance oven from 425 to 475 °C. Aging time used for each sample was 12, 24, 50, 100 and 200 h.

Table 1
Duplex stainless steel composition as received.

Duplex Stainless Steel UNS S31803							
C	Mn	P	S	Si	Cr	Ni	Co
0.018	1.480	0.019	0.001	0.450	22.220	5.590	0.130
Cu	Mo	N	Nb	Al	Sn	Ce	Fe
0.280	3.080	0.180	0.021	0.003	0.012	0.020	66.496

After aging the samples, the hardness test, for analysing the behaviour of the effect of phase transformation, was performed. After that, Charpy impact testing was accomplished in order to evaluate the energy absorbed through DSS impact, as received and in the aging conditions, and a posterior analysis of each material's fracture surface.

To study the formation of α' phase an X-ray diffraction test was performed around the peak (2 0 0), the scanning angle (2θ) varied from 63° to 65.5°, for the different treatment types. An XRD-6000 vertical type, Cu κ-α radiation, X-ray diffractometer, was used.

Ultrasonic testing was the nondestructive test used, applying the pulse echo method, with a normal V112-RM, 10.0 MHz longitudinal wave contact transducer manufactured by OLYMPUS. The tested samples' dimensions were 55 mm × 25 mm × 10 mm.

The sound speed was determined by the relation:

$$v = \frac{d}{t},$$

where d is the thickness of the sample and t is the time the ultrasonic signal takes to scan the sample's thickness and returns to the transducer. The time is determined through the overlapping of two consecutive peaks of the diagram tension *versus* time.

For the microstructural analysis of the received and aged material, the samples were prepared, polished and subjected to the electrolytic attack with oxalic acid. After this preparation, optical microscopy and scanning electron microscopy (SEM) were used to evaluate the microstructure of the received material and the fracture surfaces after Charpy impact testing.

3. Results and discussions

In this work the embrittlement kinetics of a duplex stainless steel UNS S31803, whose microstructure of the received material was obtained through optical microscopy as shown in Fig. 1, was evaluated.

3.1. Transformation of the microstructure from 425 to 475 °C

The range of temperatures are characterised by the decomposition of the $\alpha_{initial}$ phase in two phases, an α phase poor in chromium and another α' phase rich in chromium. Spinodal decomposition [13], is the mechanism responsible for this transformation. The γ phase does not suffer transformation in this region [14].

Aimed at establishing a correlation between the Rockewell C data hardness measurement, energy absorbed by Charpy impact, and aging time, graphics from these tests were obtained, as shown
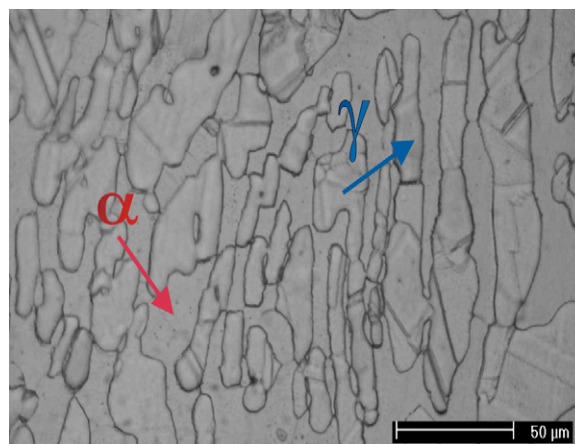

Fig. 1. Optical microscopy of the DSS as received, electrolytic attack with oxalic acid (magnification: 1000×).
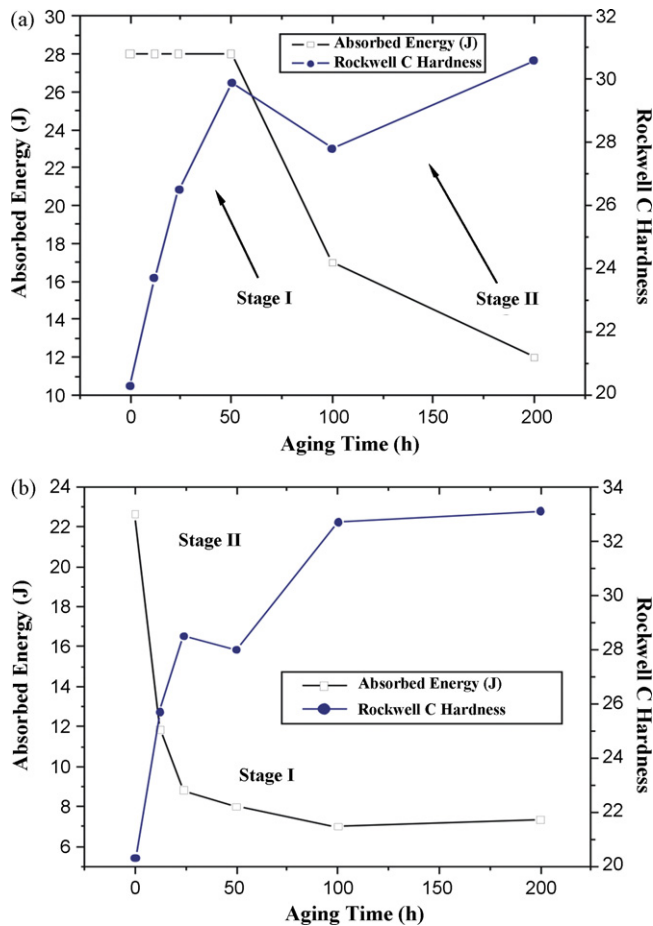
Fig. 2. Variation of the Rockwell C hardness measurements and the energy absorbed in the impact, due to the aging time at: (a) 425 °C and (b) 475 °C.

Fig. 3. Fracture Surface: (a) 50 h, and (b) 100 h of the samples treated at 425 °C (magnifications: 500×).

in Fig. 2a and b, from 425 to 475 °C, respectively. Thus, the data analysis obtained for the transformations which occurred during aging become more accurate.

Fig. 2a presents fast hardening for values up to 50 h, followed by a region of low hardening rate. The occurred hardening kinetics at 425 °C is slow. Fig. 2b, in which hardening kinetics is faster, it is observed that the hardness curve may be divided in two hardening stages, the first up to the aging time of 24 h and the second from 50 h onwards, the mechanism responsible by hardening in each stage is later analysed through X-ray diffraction. The presence of two hardening stages was observed in other works which analysed the spinodal decomposition, as in Choo et al. [15], and Kratochvil et al. [16].

In Fig. 2b, hardness increases rapidly in stage I, followed by a transition level between 24 and 50 h. After that, stage II begins with a lower hardening rate and tending to a constant value, referring to the end of α phase formation. According to Choo et al. [15], the two hardening sources responsible for stages I and II are respectively the spinodal decomposition and the growth of the particles of the ordinate phase.

The behaviour of the material due to the energy absorbed by the Charpy impact testing is shown in Fig. 2a and b. The first hardening stage is characterised by predominantly ductile fractures and microcavities, which characterise this mechanism, are observed at 425 °C, Fig. 3a. Hardening in this stage is due to the process of ferrite transformation through spinodal decomposition. The second hardening stage, which starts at 50 h, showed predominantly brittle fractures, in which he presence of its almost cleavage fracture regions is observed, as indicated, by arrows, in Fig. 3b. These frac-
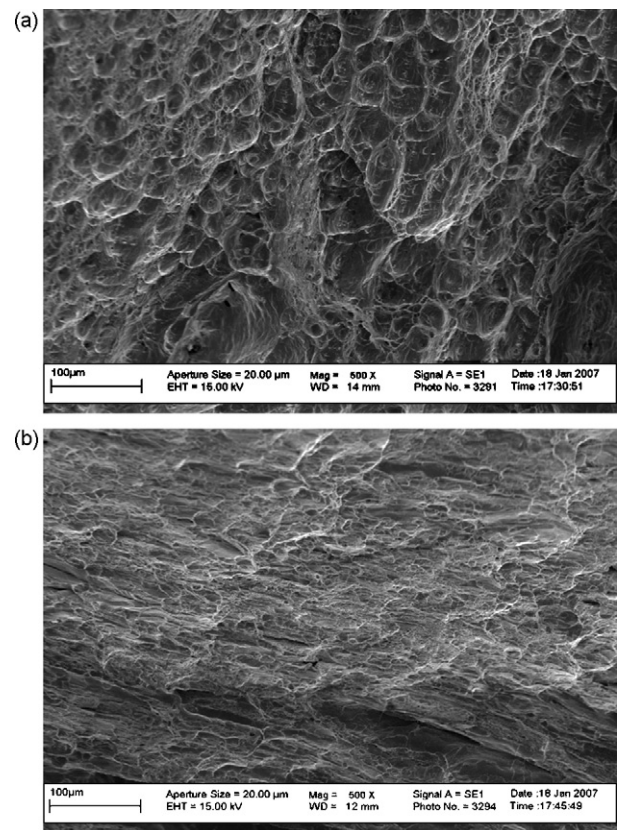
ture regions are related with the α' ordinate phases growing, which, in time, tend to line up throughout the directions $\{1\,0\,0\}$ [17].

At 475 °C, the two stages are well defined, the first stage is characterised by ductile fracture and the second by brittle fracture. This was observed at 425 °C.

The arrangement of $\boldsymbol{\alpha'}$ phase was analysed through X-ray diffraction in the peak $(2\,0\,0)$. The presence of side strips, resulting from the arrangement of phases due to the spinodal decomposition mechanism, has been observed through diffraction of the selected area through Transmission Electronic Microscopy and X-ray diffraction [17,18,19].

The peak $(2\,0\,0)$ intensity variation study reveals that samples aged at 425 °C, Fig. 4, show a peak reduction relative intensity to values up to 24 h. According to Acselrad et al. [20], this aging band corresponds to the spinodal decomposition area. However, the first stage terminates within 50 h, indicating that there are still more regions in decomposition. When this decomposition concludes, the second stage, with the growth of these particles begins. These stages, as already presented, are also observed at 475 °C.

The relative intensity reduces due to the peak's scattering $(2\,0\,0)$, as rich and poor chromium regions grow and provoke the appearance of side strips which widen the peak and reduce its relative intensity [18,21].

The phase transformations were followed-up from 425 to 475 °C through sound speed measurements. At 425 (Fig. 5a) and 475 °C (Fig. 5b), it is observed that there is a direct relationship between sound speed and hardness. This indicates that the sound speed is capable of following-up the phase transformations which occurred in the two hardening stages.

Shigeyeiki et al. [10,11], performed studies at 475 °C in duplex stainless steel samples, and found that sound speed measurements were promising to follow-up the aging kinetics at this temperature.
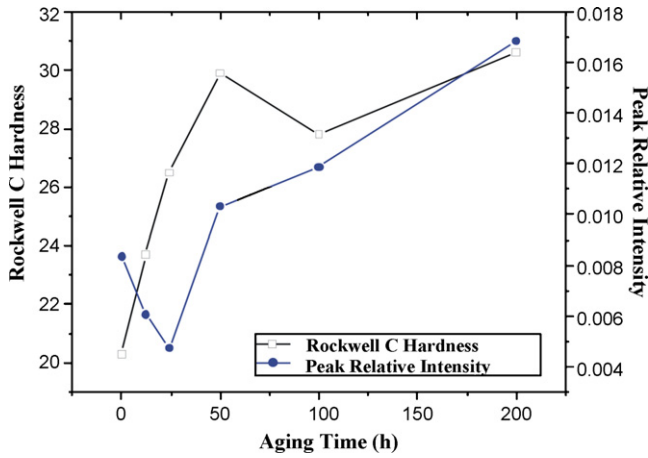
Fig. 4. Relation between peak (2 0 0) relative intensity and Rockwell C hardness for samples aged at 425 °C.

The sound speed varies inversely to the behaviour of absorbed energy. In Fig. 6a and b, an accented decline of the absorbed energy, tending to a well-defined level of brittle fracture, is observed at 425 and 475 °C, respectively. In these figures, the sound speed for samples without treatment is 5.743 m/s and it is also observed that in the brittle fracture level the speed increases to 5.786 m/s. This variation also indicates that the sound speed is sensitive to microstructures transformations.
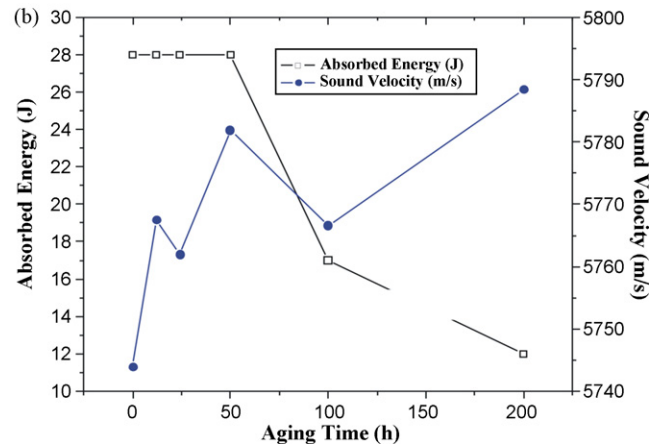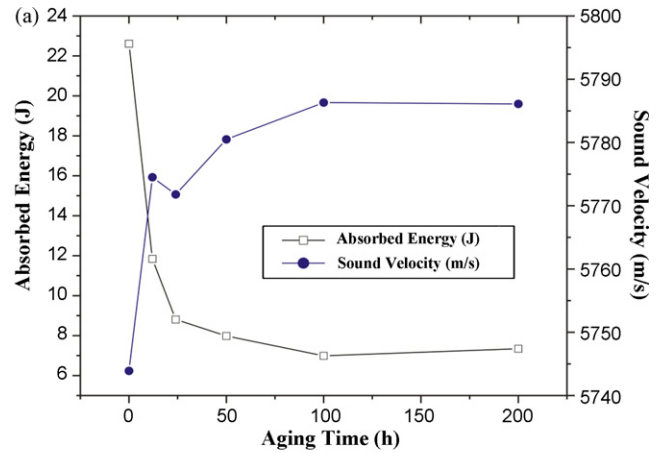

Fig. 5. Variation of sound speed and Rockwell C hardness according to aging time, at: (a) 425 °C and (b) 475 °C.

Fig. 6. Variation of sound speed due to energy absorbed in the impact, with aging time, at: (a) 425 °C and (b) 475 °C.
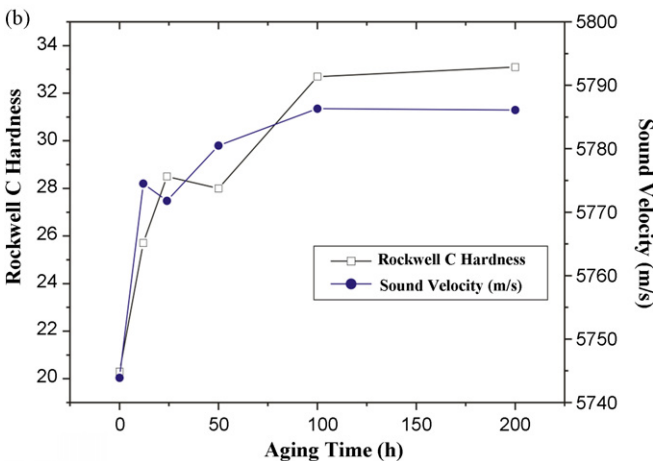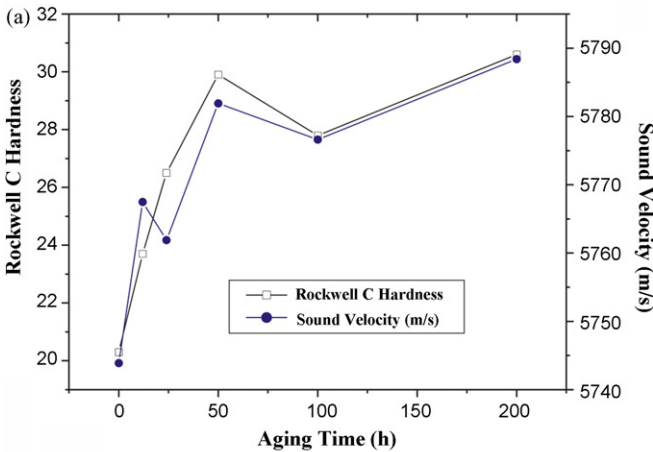
Badidi et al. [22], observed that the microstructure variation and hardness are correlated with the sound speed and regarding the thinner steel microstructure, the larger is the contours surface quantity, increasing the material's hardness and consequently the sound speed will be greater.

In materials where the microstructural transformation is caused by the spinodal decomposition mechanism, during decomposition of the α′ phase there is a formation of alternate regions rich and poor in chromium. Regions enriched in chromium are responsible for the rigidity alteration of the iron matrix, provoking the increase of sonic speed values. When the first period concluded, the spinodal decomposition region ends and the α′ phase growth begins, this α′ phase is consolidated at the end of the second hardening stage. With that, the rigidity becomes constant, and a baseline for sound speed values is observed.

4. Conclusions

The UNS S31803 duplex stainless steel embrittlement study was performed in the band of 425 and 475 °C. The transformations' analysis was based on X-ray diffraction measurements, optical microscopy, scanning electron microscopy, sound speed measurements, Charpy impact and hardness tests.

The observations performed allowed the following conclusions:

(1) The studied duplex stainless steel showed two hardening stages. The first hardening stage is characterised by the spinodal decomposition mechanism and the second by the growth of the formed phases.

(2) The first hardening stage is characterised by ductile fracture and the second shows low levels of absorbed energy and predominance of brittle fracture, characterising an embrittlement region of the material.

(3) The variations of the sound speed measurements are directly proportional to the variation of the material's hardness measurements, showing sensitivity to the transformation phases. Thus, the sound speed is an important nondestructive parameter for following-up the hardening kinetics of duplex stainless steel.

Acknowledgments

References

[1] S.E. Kruger, J.M.A. Rebello, P.C. de Camargo, NDT&E International 32 (5) (1999) 275–281.
[2] M.D. Russel, The Journal of the Acoustical Society of America 3 (1993) 1267–1276.
[3] S.E. Kruger, Aplicação da análise espectral de ecos e do sinal retro espalhado na detecção de danos por hidrogênio em aços, in: XIV Congresso de Pesquisa e Inovação da Rede Norte Nordeste de Educação Tecnológica, 1995, pp. 72–79.
[4] S. Bhattacharyya, M.B. Das, S. Sarkar, Engineering Failure Analysis 15 (6) (2008) 711–722.
[5] M.S. Kumar, M. Sujata, M.A. Venkataswamy, S.K. Bhaumik, Engineering Failure Analysis 15 (5) (2008) 497–504.
[6] H. Berger, Materials Evaluation 50 (2) (2000) 299–305.
[7] S.S.M. Tavares, R.F. Noronha, M.R. Silva, J.M. Neto, S. Pairis, Materials Research 4 (4) (2001) 237–240.
[8] A. Badidi, A. Benchaala, K. Alem, Ultrasonics 38 (2000) 224–227.
[9] M. Tane, T. Ichitsubo, H. Ogi, M. Hirao, Scripta Materialia 48 (2003) 229–234.
[10] H.W. Shiegeyuki, International Conference on Nuclear Engineering 5 (2000) 215–223.
[11] M. Shigeyuki, M. Hiroshi, M. Kazuhiro, S. Jun, I. Takuichi, M. Kumada, Y. Kurosumi, Y. Okano, International Conference on Nuclear Engineering 5 (1996) 215–223.
[12] P. Palanichamy, A. Joseph, T. Jayakumar, B. Raj, NDT&E International 28 (3) (1995) 179–185.
[13] F. Iacoviello, F. Casari, S. Gialanella, Corrosion Science 47 (4) (2005) 909–916.
[14] M.D. Mathew, L.M. Lietzan, K.L. Murty, V.N. Shah, Materials Science and Engineering A 269 (1) (1999) 186–196.
[15] W.K. Choo, H.J. Kim, J.C. Yoon, Acta Materialia 45 (12) (1997) 4877–4885.
[16] P. Kratochvíl, J. Mencl, J. Pešička, S.N. Komnik, Acta Metallurgica 32 (9) (1984) 1493–1500.
[17] A.M. Mebed, T. Koyama, T. Miyazaki, Computational Materials Science 14 (1–4) (1999) 318–322.
[18] T. Miyazaki, T. Koyama, Materials Transaction JIM 37 (4) (1996) 684–690.
[19] N. Mattern, G. Goerigk, U. Vainio, M.K. Miller, T. Gemming, J. Eckert, Acta Materialia 57 (3) (2009) 903–908.
[20] O. Acselrad, I.S. Kalashnikov, E.M. Silva, M.S. Khadyev, R.A. Simao, Metal Science and Heat Treatment 48 (11–12) (2006) 543–553.
[21] I.S. Kalashinikov, V.D. Kibalnik, V.S. Litvinov, Y.E.I. Maliyenko, Structure and properties of non-magnetic steels (1986) 83–88.
[22] A. Badidi, S. Lebaili, A. Benchaala, NDT&E International 36 (1) (2003) 1–5.